

# Chapter 4

*In vitro* and *in silico* interaction of  $\alpha$ -amylase and  $\alpha$ -glucosidase with *Daruharidra* extract and evaluation of antidiabetic activity.

## **Chapter 4**

### ***In vitro* and *in silico* interaction of $\alpha$ -amylase and $\alpha$ -glucosidase with *Daruharidra* extract and evaluation of antidiabetic activity.**

#### **4.1 Background-**

Various plants and their extracts have demonstrated promising antidiabetic properties, including inhibition of alpha-amylase and alpha-glucosidase as a key enzyme involved in carbohydrate digestion. For instance, in this chapter *Daruharidra* plant, has been investigated for its ability to inhibit alpha-amylase activity. *Daruharidra* (*Berberis aristata*), known for its potential medicinal properties. The alcoholic extracts exhibited potent inhibition of alpha-amylase and alpha-glucosidase indicating their potential as natural antidiabetic agents. This inhibitory effect and antioxidant potential of *Daruharidra* extracts have been evaluated in this chapter using *in vitro* assays. Furthermore, molecular docking studies have identified specific phytoconstituents from *Daruharidra*, such as berbamine and alloxanthine, which show strong interactions with alpha-amylase, suggesting their potential as therapeutic agents for diabetes management. These assays included enzyme kinetics studies, % glucose uptake by yeast cells assay, and assessment of superoxide dismutase activity. Moreover, enzyme kinetics studies have revealed that ethanolic extracts exhibit an IC<sub>50</sub> value indicative of significant inhibitory activity against alpha-glucosidase, with a competitive mode of inhibition. The methanol, acetone, and ethanol extracts showed the lowest IC<sub>50</sub> values for alpha-amylase inhibition, with a non-competitive mode of inhibition.

Among the numerous compounds identified, a few phytochemicals were selected for docking studies. For alpha-glucosidase and alpha-amylase, respectively, protein-ligand complex stability was evaluated using molecular dynamics (MD) simulations across times of 100 and 150 nanoseconds. When juxtaposed with the reference chemical Acarbose, the complexes

showed exceptional stability. The screened ligands demonstrated strong binding energies with alpha-amylase and alpha glucosidase indicating significant inhibitory activity. These findings suggest promising potential for the *Daruharidra* plant extracts as enzyme inhibitors, warranting further in vitro validation.

The results of these experiments have shown that *Daruharidra* extracts possess the ability to inhibit alpha-glucosidase activity, thereby reducing the absorption of glucose through the plasma membrane of yeast cells. The focus of this study is to investigate the potential of the *Daruharidra* plant (stem and bark) in inhibiting alpha-amylase and alpha-glucosidase activity to establish it as potent antidiabetic agent. These findings underscore the potential of *Daruharidra* extracts and their constituents as effective therapeutic agents for diabetes management, offering novel avenues for the development of effective and sustainable therapies for this chronic condition.

#### **4.2 Introduction-**

The prospect of using *Daruharidra* to treat diabetes is being continuously explored. *Daruharidra* or *Berberis aristata* is a plant whose fruits and other parts are used for the prevention of much drug-related toxicity. Efforts in this article are directed to study the activity of *Daruharidra* in inhibition of the alpha-amylase enzyme. Alpha-amylases are starch hydrolyzing enzymes that give several products upon hydrolysis like dextrans and small polymers of glucose units leading to high blood glucose levels, as in the case of type 2 diabetes mellitus.[109] Inhibitors of this enzyme maintain postprandial glucose level by delaying digestion and absorption of intestinal sugars.[49] Standard treatment for diabetes type 2 can be done by reducing insulin demand in the body, inhibiting the digestion of carbohydrates like in the case of alpha amylase inhibition or just increasing insulin reaction at target sites. [110] According to WHO, Diabetes caused an estimated 1.6 million deaths worldwide in 2016 and according to national diabetes report in 2017 diabetes became 7<sup>th</sup> leading cause of death in

America.[111] Diabetes is known as a significant cause of blindness, kidney failure, heart attacks, stroke, and lower limb amputation. [112]. Reports show the hepatotoxicity caused due long-term medications for tuberculosis where berberis fruit extract was used to cure paracetamol and CCl<sub>4</sub> induced hepatic damage. [136] Tonic remedy made for liver and heart patients from *Daruharidra* extract also proves helpful in many cases. [137].

In some studies, it's seen that aqueous extract of the plant causes a positive antidiabetic effect, lowers total cholesterol, and significantly increases HDL-C levels. *Daruharidra* can also cause a reduction in obesity. [138]. The alcoholic extract of roots of this plant can decrease gluconeogenesis and thus maintain glucose homeostasis in our bodies. [139] Research is conducted on this polygenic illness, wherein Acarbose, when combined with postprandial hypoglycaemic drug therapy, helps to reduce postprandial glucose variations. This sugar will be used by the body in early stages of type two diabetes or in prediabetes conditions.

Apart from Acarbose, which is as such not obtained from plants, comes from its precursor molecule which is produced by the microorganism Actinoplanes.[140] *Daruharidra* has abundance of phytochemicals which includes phenols, flavonoids tannins and alkaloids. We focussed our study on alkaloids which are known to be a class of spontaneously occurring chemical constituents having pronounced pharmacological activities. This article wished to conclude that there are many compounds of alkaloidal nature still unexplored that can be utilised to more successfully combat diabetes and its associated consequences by repurposing a new, promising medicine. The goal of the current research was to assemble comprehensive data on naturally occurring alkaloids that have the ability to block the alpha-glucosidase enzyme.

### 4.3. Methodology

#### 4.3.1 Chemicals utilized-

Alpha-amylase (porcine pancreas) was obtained from Sigma Aldrich, while soluble starch (extra pure) was the product of Himedia. Alpha-glucosidase enzyme from yeast and its substrate p- nitrophenyl alpha-D-glucoside (PNPG) were procured from Sisco research laboratories SRL.

#### 4.3.2 Percentage Glucose uptake through yeast plasma membrane-

For the experiment commercial bakers' yeast was procured. It was washed with distilled water three times and centrifuged (3000g, 5 min). Yeast suspension (10% v/v) was prepared in Mili Q water. Glucose solution was prepared by adding 100mg glucose to 100 ml distilled water. The reaction mixture contained varying amounts of plant extracts (2-20mg) preincubated with 1ml of a glucose solution for 10 min. The reaction was initiated by adding, 100µl of prepared yeast mixture, which was then added to the above solution. [142]The preparation was vortexed, and set aside for incubation at 37°C for 1 hour. The tubes were centrifuged at 3000g for 5 min. The supernatant was taken to estimate the remaining amount glucose using a spectrophotometer at 520 nm and the percentage increase in glucose uptake by yeast cells was calculated.

$$\frac{\text{Absorbance (control)} - \text{Absorbance (sample)}}{\text{Absorbance (control)}} * 100$$

#### 4.3.3 Inhibitory effect of *Daruharidra* extract on alpha-amylase inhibition

500 µl of extract (2–12 mg/ml) were added to a tube along with 500 microliters of 0.02M sodium phosphate buffer (pH 6.9) that included a solution of α-amylase (2U/mL). After preincubating this solution for 10 minutes at 25°C, 250 µL of a 0.5% starch solution in 0.02M sodium phosphate buffer (pH 6.9) was added and the mixture was once again incubated for 10 minutes at 25°C. Add 500 µL of the dinitrosalicylic acid (DNS) reagent to stop the process.

After five minutes of incubation in boiling water, the tubes were allowed to cool to room temperature. A spectrophotometer was used to detect the absorbance at 540 nm after diluting the reaction mixture with 5 mL of distilled water. [129] Prepare a control using the same procedure replacing the extract with distilled water. Calculated the  $\alpha$ -amylase inhibitory activity as percentage inhibition:

$$\text{Inhibition}\% = \left( \frac{AB_{\text{control}} - AB_{\text{extract}}}{AB_{\text{control}}} \right) * 100$$

#### **4.3.4 Mode of inhibition of alpha-amylase-**

The lowest IC<sub>50</sub> concentration extract is taken for the mode of inhibition assay. As acetone and methanol extracts reported the lowest IC<sub>50</sub> values, we used Michaelis-Menten and Lineweaver-Burk equations for the calculation of mode of inhibition of alpha-amylase. [130] This IC<sub>50</sub> concentration (mg/ml) of methanol and acetone extracts gave results for enzyme kinetics studies. Organize two sets of reaction with the former having 250 $\mu$ l of plant extract preincubated with an alpha-amylase enzyme (2U/ml) for 10 min @ 25°C and later having 250 $\mu$ l of buffer in place of extract rest remaining same. Soluble starch solution 250 $\mu$ l in increasing concentration (0.1-5mg/ml) added as a substrate to both sets of reactions. Incubate the reaction for 10 mins. Stop the enzymatic reaction by using 1 ml DNS reagent and let them boil for 5 mins. Spectrophotometric estimation of the amount of reducing sugars was performed by translating the maltose standard curve into reaction velocities. From the slope and intercept values in double reciprocal plots, the kinetic constants Km and Vmax were determined. Using maltose as a standard, the concentration of the product (reducing sugars) was calculated and reported as millimoles of equivalent.

#### **4.3.5 Inhibitory activity of *Daruharidra* extract on alpha-Glucosidase enzyme.**

The enzyme inhibition reaction was carried out on the alpha-glucosidase enzyme. Inhibition potential was determined using the modified method of Kim et al. [131] 1U/ml of  $\alpha$ -glucosidase mixed with 10ml phosphate buffer (20mM, pH 7.0). The reaction consisted of 50  $\mu$ L of plant extract at varying concentrations (2- 20mg/mL). 450  $\mu$ L phosphate buffer pH 7.0 and 50  $\mu$ L of 3 mM PNPG substrate p-nitrophenyl  $\alpha$ -D-glucopyranoside. The extracts were previously incubated with the enzyme, (37°C,15 min) to initiate the inhibition, PNPG was added to each tube to start the left-over enzyme-substrate reaction. The reaction was terminated by adding 2ml Na<sub>2</sub>CO<sub>3</sub> (0.1M). Enzyme activity was observed as measure of absorbance with help of spectrophotometer at 405 nm. Well-known alpha-glucosidase inhibitor acarbose was taken as a positive control. The extract's IC<sub>50</sub> value was the concentration needed to block 50% of - glucosidase activity under the assay's predetermined conditions.

$$Inhibition\% = \left( \frac{AB_{control} - AB_{extract}}{AB_{control}} \right) * 100$$

#### **4.3.6 Mode of inhibition assay for alpha glucosidase enzyme -**

Alpha-glucosidase was preincubated with IC<sub>50</sub> concentration of plant extract in 50mM Tris-HCl buffer (pH 7.0) at 25°C.[49][143] The reaction mixture contained varying amounts of substrate PNPG. The quantitative estimation of reducing sugar was done using a p-nitro phenol standard curve, which was further converted to reaction velocities. Inhibition type was analyzed by the double reciprocal (Lineweaver-Burk) plot. It was calculated from the result according to the Michaelis-Menten kinetics. [144]

#### **4.3.7 Docking of alpha-amylase on HRLC/MS screened ligands-**

Screened ligands shortlisted by hits resulting from HRLC/MS for molecular docking for their probable anti-diabetic effect as alpha-amylase inhibitors were mainly alkaloids.[131] All ligands were docked on target enzyme alpha-amylase PDB ID PIF 1. The structure of enzymes and ligands was obtained from the Protein Data Bank, RCSB database, and National Centre for Biotechnology Information, PubChem database (<https://pubchem.ncbi.nlm.nih.gov/>) was used, respectively. [132]The active site of the enzyme obtained from the FT server showed amino acid TRP A 329, ASP A 357, ILE A 358, ILE A 396, ASP A 398, and ARG A 624 on the active site. [133] AutoDock 4.2 open-source software was used for docking and creating a grid center box. In the docking study, the ligand molecule was kept flexible and the enzyme very rigid. Marvin suit (Chemaxon Marvin,2019) and PyMol (Biovia, 2017). software were used to prepare structures and visualize the result. Interaction analysis was done by Discovery studio.

#### **4.3.8 Molecular dynamic simulation studies of PIF1 and docked ligands-**

Molecular dynamics is a method to explore the structure of compound/solid by using classical mechanics and generating trajectory. Gromacs 2020 has been used for MD, which uses the concept of periodic boundary to form boxes /grids and groups to show action. After the arrangement of information, topology was generated using AMBER99SB force field for protein and Gaff force field for ligand. 4Na were added for neutralization, and then steric clashes were removed. The steepest descent algorithm achieved energy minimization until the maximum force went below 1000KJ/mol/nm. After this, the system was subjected to solvation using the TIP3 water model. All complexes were submitted for 150 for PIF1 and ligands in MD simulation. At the end of the simulation, the Root Mean Square Deviation (RMSD), Root Mean Square Fluctuation (RMSF), and RG (radius of gyration) were calculated. Post-MD simulation analysis calculated Solvent Accessible Surface Area (SASA). Principal component analysis

(PCA) for detecting the direction and amplitude of the dominant motions.[134]. GBSA (generalized born surface area) was done for the last 15ns. The number of H-bonds was calculated by using Gromacs utilities.

#### **4.3.9 Docking of phytochemicals hits found in HRLCMS on alpha-glucosidase**

Referring to the experiments performed and hits observed in HR-LCMS, the phytoconstituents mainly found were naturally alkaloid. Each hit was searched on the PubChem database (<https://pubchem.ncbi.nlm.nih.gov/>). Structure and chemical properties of observed alkaloids were found and their 3-dimensional structures downloaded from the website. All the alkaloids were subjected to docking on target enzyme i.e., human lysosomal alpha-glucosidase PDB ID 5KZX. Enzyme's 3-dimensional structure was procured via the Protein Data Bank, RCSB database, and National Centre for Biotechnology Information. Using the weighted rotor search for lowest energy conformer option in the Open Babel tools (<http://openbabel.org>), ligands in SDF format were converted to PDB file format.

Using Raccoon software, all ligands were assigned to the addition of polar hydrogen, the computation of Gasteiger charges, and the control of the torsion tree by selecting the root prior to molecular docking. The ligand files were saved in the pdbqt format.[145],[146].The enzyme's active site was obtained from the open-source FT site server (<https://ftsitesite.bu.edu/>) provided by Vajda labs at Boston University. Active site contained ILE 441, TRP 516, PHE 649, TRP 376, ASP 404, HIS 674, ASP 443.[133] An open-source software AutoDock 4.2 was employed to make the grid center box. The BIOVIA Discovery Studio Visualizer (<http://3dsbiovia.com/products/>) was used to generate the protein. (DeLano, 2002) and PyMol (Biovia, 2017). After eliminating ions, water molecules, cofactors, and ligands, the protein structure was stored in PDB format for later examination. Using AutoDock technologies, polar hydrogen atoms were introduced to the protein. Subsequently, the cleaned protein was

subjected to energy minimization using Swiss PDB Viewer software, employing the GROMOS-14B1 forcefield. [147] All the hits were docked with the alpha glucosidase enzyme. In X, Y, and Z dimensions, the number of grid points was fixed at  $127 \times 127 \times 127$ , and the default grid spacing for the protein was 0.800 Å. The box was placed in the middle of the active site pocket, which included all of the binding site residues and gave the ligands room to move both translationally and rotationally. For ten distinct GA runs, the Lamarckian genetic algorithm was applied with the following specifications: a maximum of 27,000 generations, a population size of 150, and a maximum energy evaluation of 2,500,000. For the structure preparation Marvin suit software (Chemaxon Marvin,2019) was used and PyMol (Biovia, 2017). was utilised to display the outcome. [148]

#### **4.3.10 Molecular dynamic simulation studies of 5KZX and ligands-**

A technique for investigating the structure of a compound or a protein by employing classical mechanics with generating its trajectories is a widely explored area known as Molecular dynamics MD. Gromacs 2020, which uses the periodic boundary idea to create boxes, grids, and groups to represent activity, was made available for this study's MD. The stability of the compound was analyzed using molecular dynamic simulation, which ran 4000 frames for 100 ns at time steps of 25 Pico seconds. Using GROMACS, the AMBER99SB force field was acquired in order to determine the topology of proteins. However, ACPYPE was used to achieve the GAFF force field for ligands. Using the TIP3P water model, the complex was solvated in a dodecahedron box measuring  $113.1177 \times 113.1177 \times 79.9863$  Å. Two Na ions were then added to neutralize the system while preserving at least 10 Å of space between the protein edge and the box boundary. The system's energy was reduced and steric conflicts were eliminated until the highest force was less than 1000 kJ/mol/nm. In addition to incorporating NVT and NPT at 100 ps each, the temperature was kept at 310 K and the pressure was kept at

1 atm. The Root Mean Square Deviation (RMSD), H bond was calculated using Gromacs utilities. Root Mean Square Fluctuation (RMSF) and RG (radius of gyration) were calculated for the complexes at the end of the simulation. Solvent Accessible Surface Area was calculated using post-MD simulation analysis (SASA). [134]

#### **4.3.11 Drug likeness prediction/ ADMET analysis–**

To investigate pharmacokinetic properties of all the 24 ligands and their drug likeness index as probable leads SWISS ADME (<http://www.swissadme.ch/>) online tool was employed. It made it easier to comprehend effectiveness of the leads and if they could be taken further for assessment as a potential drug. [149]FDA or other regulatory agencies prefer potential leads that exhibit satisfactory ADMET (absorption, distribution, metabolism, excretion, and toxicity) parameters for easy approval as new drugs in the market. To calculate the individual ADME behaviors of the compounds from *Daruharidra*, a web server displaying the Swiss ADME Submission page allowed access to the Swiss ADME program from the Swiss Institute of Bioinformatics. The list is designed to have a single-entry molecule per line with multiple inputs which is specified by SMILES also known as simplified molecular input line entry system.[150] The toxicity profile of the leads was studied by ProTox online server. The Lipinski rule of 5 was kept in mind while analysing the results, and the toxicity analysis was known by online LD50 prediction tool PROTOX II ([tox-new.charite.de](http://tox-new.charite.de)).[151][152], [153]

### **4.4 Results and discussion**

#### **4.4.1 Percentage glucose absorption by yeast cells-**

The plant extracts' adsorption abilities were shown to be directly related to the increasing molar concentration of glucose used. It was observed that larger amounts of glucose were bound with higher glucose concentrations. The rate of glucose uptake into yeast cells was found linear for

the concentration employed in the study.[142][159] The quantity of glucose that remains in the media after a certain period serves as an indicator of how much glucose the yeast cells have consumed.

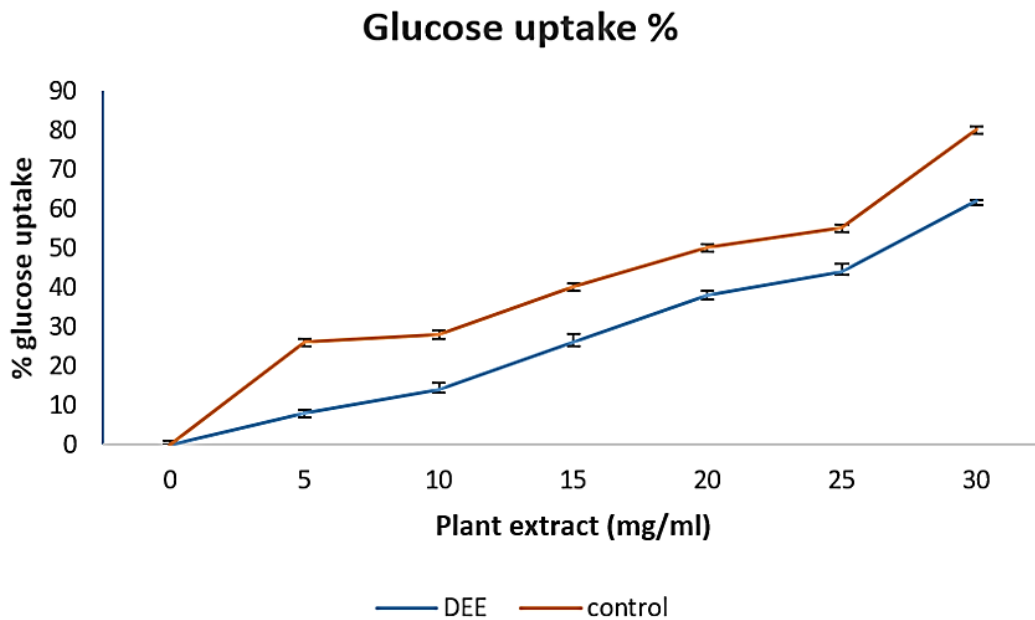


**Figure 4.1.** The effect of *Daruharidra* ethanolic extract (DEE) on glucose uptake by the yeast cell at different plant concentrations.

According to the report's results, ethanolic bark and stem extract improved yeast cells' ability to absorb glucose at different plant extract concentrations. A measure of how much glucose the yeast cells have consumed over a period of time is the quantity of glucose still present in the medium. Current research on the transport of sugars that cannot be metabolized and glycosides leads to the conclusion that stereospecific membrane carriers mediate sugar transport across yeast cell membrane. According to reports, the method by which glucose is carried in yeast cells is exceedingly complicated, although it's generally accepted that this process involves assisted diffusion. Figure 4.1. Yeast cell glucose absorption is determined by how much glucose is still present in the medium after a specific length of time. As a conclusion, this study raises

the possibility that an increase in glucose transport across cell membranes serves as an anti-hyperglycaemic action mechanism.[160]

#### 4.4.2 Alpha-amylase inhibition-

Amongst eight extracts methanol, ethanol and acetone extracts had the lowest IC<sub>50</sub> of 5.554mg/ml, 7.321mg/ml and 6.576mg/ml respectively. These three extracts were further chosen for kinetics studies of enzyme inhibition. (Table 4.2) Reaction velocities were calculated using maltose standards at different concentrations of substrate. The mode of inhibition was determined by the Lineweaver Burk plot, which revealed the inhibition type being non-competitive, shown in Figure 4.2. Table 4.2.

**Table 4.1** Alpha-amylase inhibition assay.

<b>Solvents</b>	<b>IC<sub>50</sub> mg/ml</b>
Water	8.129 ± 0.170
Methanol	5.554 ± 0.216
Ethanol	7.321 ± 0.223
Isopropanol	8.75 ± 0.121
Acetone	6.576 ± 0.320
Chloroform	11.34 ± 0.236
Pet. ether	16.68 ± 0.281
Hexane	22.52 ± 0.307

**Table 4.2** Kinetic constants,  $K_m$  and  $V_{max}$  of  $\alpha$ -amylase enzyme with and without extracts.

	$K_m$	$V_{max}$	Type of inhibition
<b>Enzyme without inhibitor</b>	0.1510	5.848	
<b>Enzyme with methanol extract</b>	0.2050	5.128	Non-Competitive
<b>Enzyme with ethanol extract</b>	0.149	3.239	Non-competitive
<b>Enzyme with acetone extract</b>	0.1453	3.85	Non-competitive

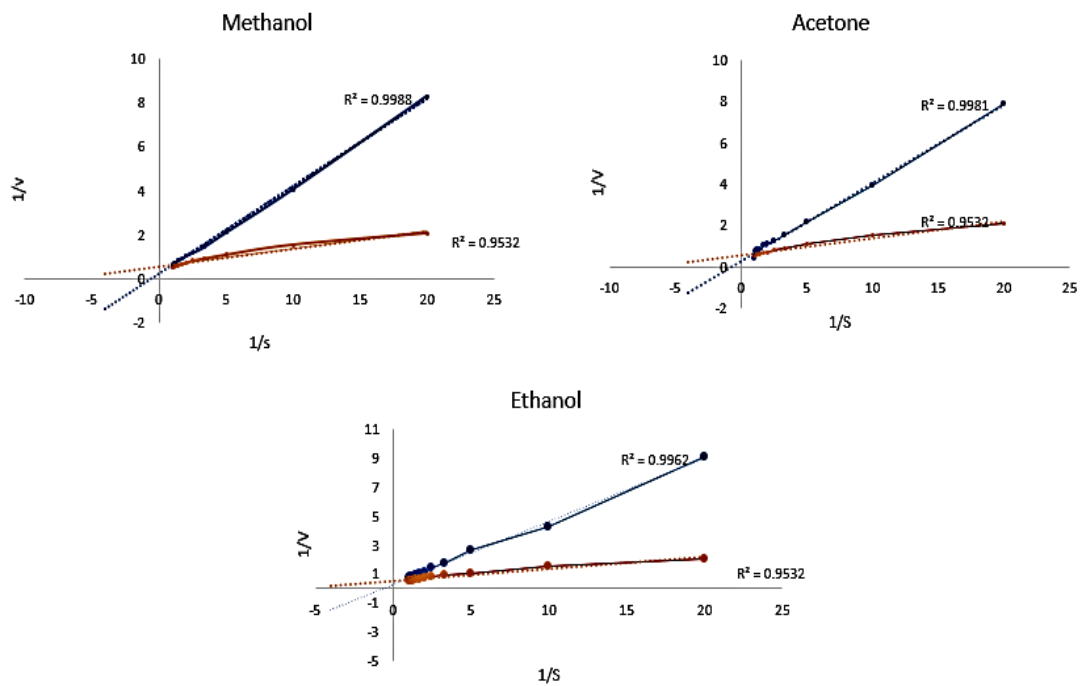


**Figure.4.2** Lineweaver Burk plot of methanol, ethanol, and acetone showing non-competitive inhibition effect on enzyme alpha amylase action on incubating in the 250  $\mu$ L extract for 10 minutes at 25°C, of a 0.5% starch solution.

#### 4.4.3 Docking studies on alpha-amylase-

All the ligands were docked on the allosteric site of the alpha-amylase enzyme. The in vitro research indicates that the *Daruharidra* extract exhibits non-competitive inhibition. To determine the shortlisted hits' enzymatic binding affinity, docking was used. Table 4.3 indicates the binding energy for the optimal blind docking pose. Among all the positions, the one with the least binding energy was selected as the optimal binding stance. The optimal stance was photographed, as shown in Figure 4.3. When compared to other ligands, berbamine exhibits the highest binding affinity against the a-amylase enzyme. It interacts with several residues and establishes hydrogen bonds with LYS200, ASP 197, and ASP 300. It was discovered that the binding energy value was -9.28 kcal/mol.

**Table 4.3** Docking details of different ligands on alpha amylase.

Ligands	Binding energy (kcal/mol)	H bonds	Amino acids	Binding site coordinates
Berbamine	-7.70	3	ARG, ARG, ASP	(94.74, 54.47,12.24)
Benazepril	-8.00	4	ASP, THR, ASN, ASN	(76.50,21.76,21.32)
Chelidonine	-8.40	3	THR, GLU, SER	(87.59, -0.66,10.52)
Alloxanthin	-7.20	6	ASP, ASP, TRP, ARG, ASP, HIS	(-2.07, -9.44, -21.22)
Procaine	-5.90	5	SER, GLN, SER, SER, GLY	(96.93,20.35, 1.16)
Protopine	-8.00	3	ASP, ASP, TRP	(103.80,19.38,29.36)
Tiagabine	-7.00	4	SER, SER, GLN, SER	(95.95,19.72, -0.61)
Colforsin	-6.30	3	LYS, ASN, GLU	(118.38,53.96,6.55)
Nadolol	-7.00	6	SER, ASP, ASN, GLU, SER, TYR	(77.89,21.04,21.14)
Evoxine	-7.50	4	ASP, ASN, ARG, ARG	(96.66, 23.20, 5.18)

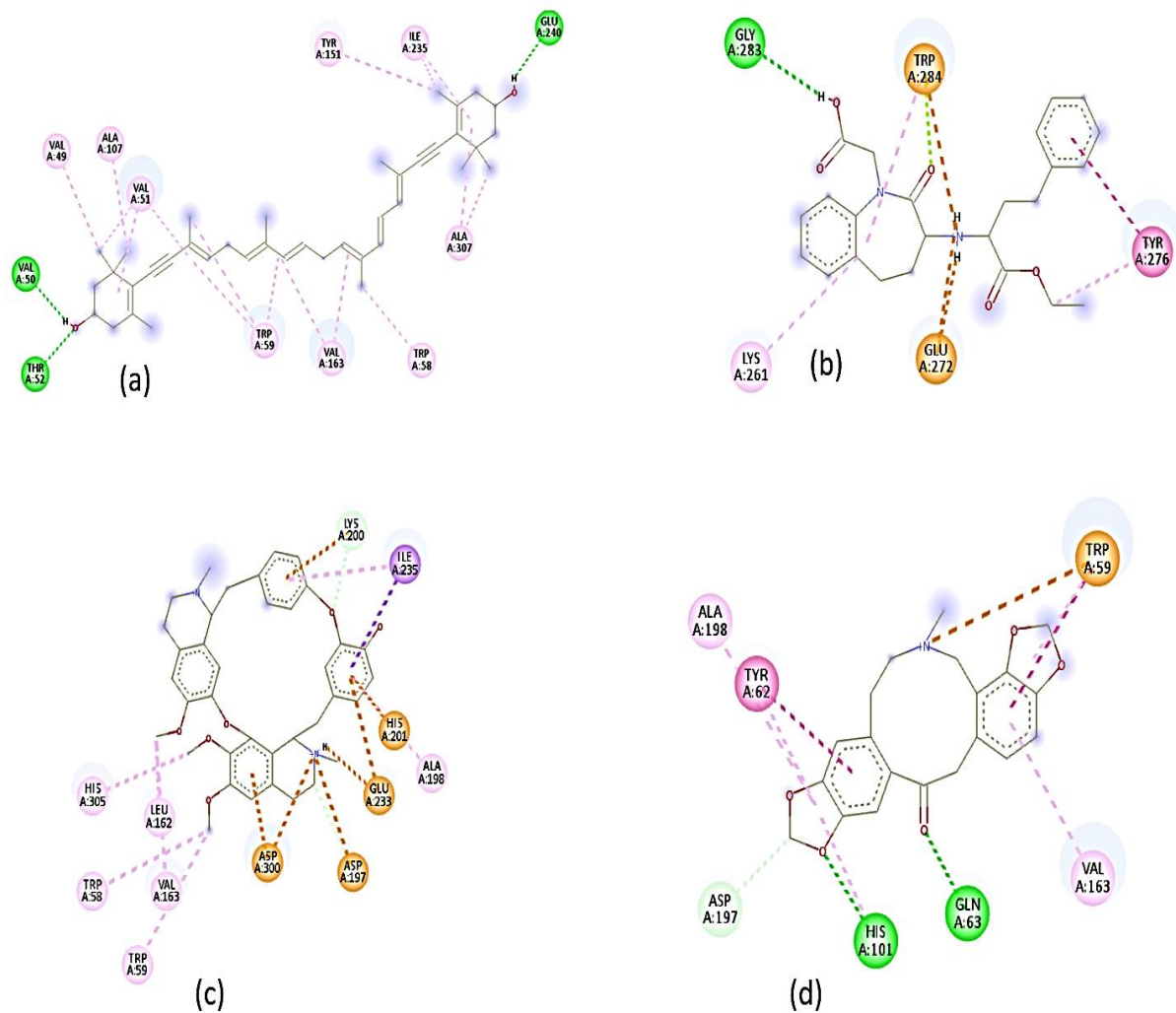


**Figure.4.3** Images of Docked ligands (a) alloxanthine, (b) benazepril, (c) berbamine, (d) protopine on alpha-amylase

#### 4.4.4 Simulation studies on alpha-amylase-

Alpha-amylase and ligands were subjected for MD simulation analysis to determine the structural stability of the complexes as described above in methods, whereas Acarbose was used as control. The RMSD, RG, RMSF, hydrogen bond, and SASA calculations analyzed structural changes in complex and dynamic behaviour. The RMSD (root mean square deviation) plot of native  $\alpha$ -amylase and protein-ligand complexes (Figure 4.4) were calculated for all complexes for 150 ns trajectory.

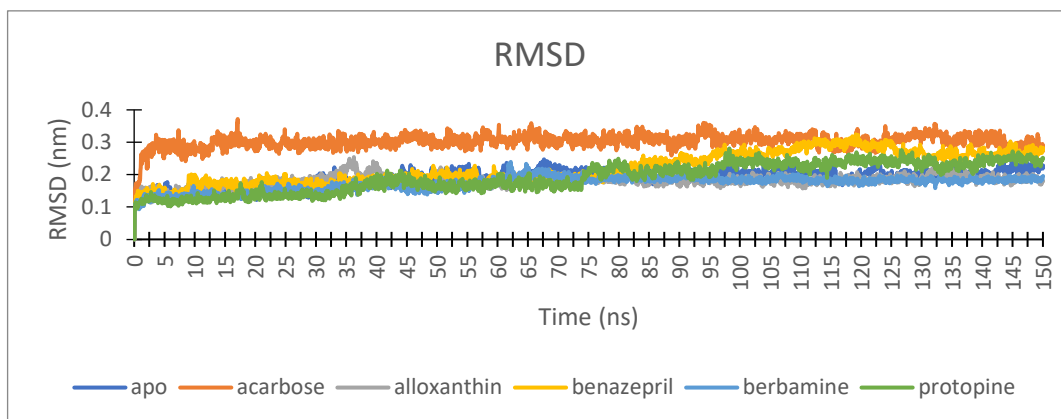


**Figure 4.4** RMSD study plot of alpha-amylase enzyme (Apo) and screened ligands with control (Acarbose).

Simulation studies show that Acarbose has a minimum RMSD standard, which implies tight binding between ligand and receptor alpha-amylase. Protopine has less close binding evident by non-overlapping RMSD, followed by benazepril and berbamine, which have close to control binding. Acarbose gets stabilized after 15ns, and berbamine is shown to get stable after 70ns. The RG value was calculated by using a 150 ns trajectory. Figure 4.6 shows the plot of average RG as a function of time for native protein and all the a-amylase-ligand complexes. The fluctuations in the constituent residues were observed for enzyme a-amylase and all the protein-ligand complexes (a-amylase-Acarbose, a-amylase-berbamine, a-amylase-alloxanthin, a-amylase- benazepril, a-amylase-protopine) were plotted as a function of time during 150 ns trajectories of MD simulation in Figure 4.5. All the complexes showed similar RMSF values and fluctuations in the identical residues. SASA calculation predicts the extent of the conformational changes during the interaction. Figures 4.6 and 4.7 show H bond and SASA values vs. time for all the protein a-amylase-ligand complexes, respectively.

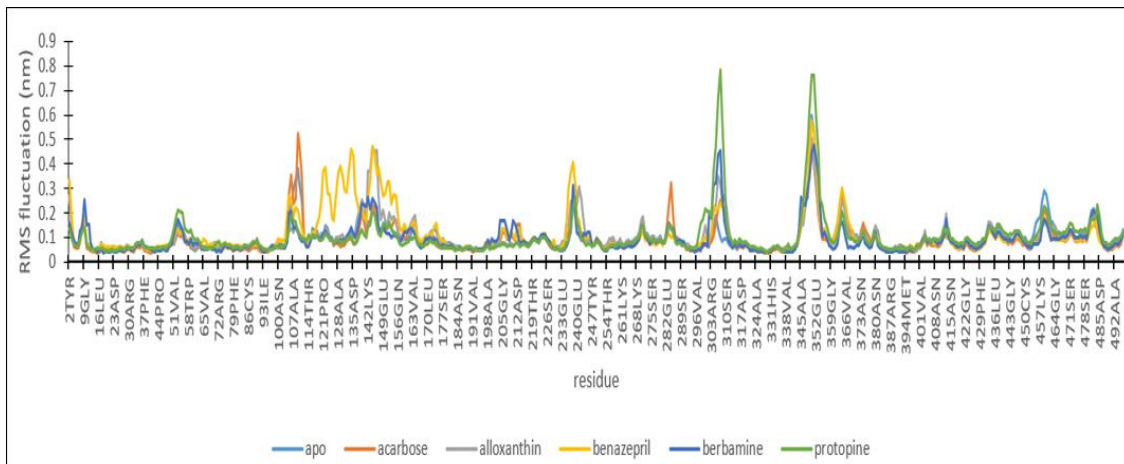


**Figure 4.5.** The RMSF values of the alpha-amylase enzyme and all protein-ligand complexes.

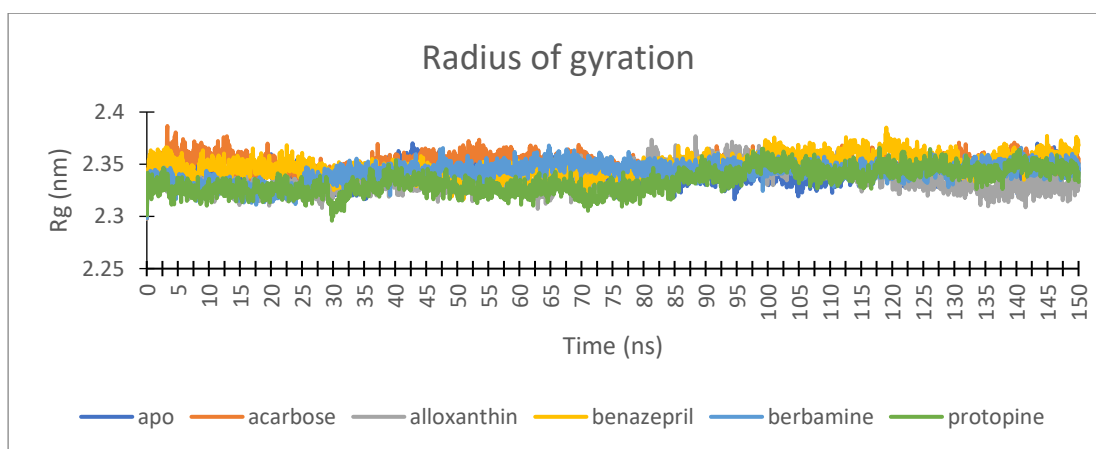


**Figure 4.6.** Radius of Gyration plot depicting the changes observed in the conformational behavior of the alpha-amylase enzyme (apo) and all protein-ligand complexes

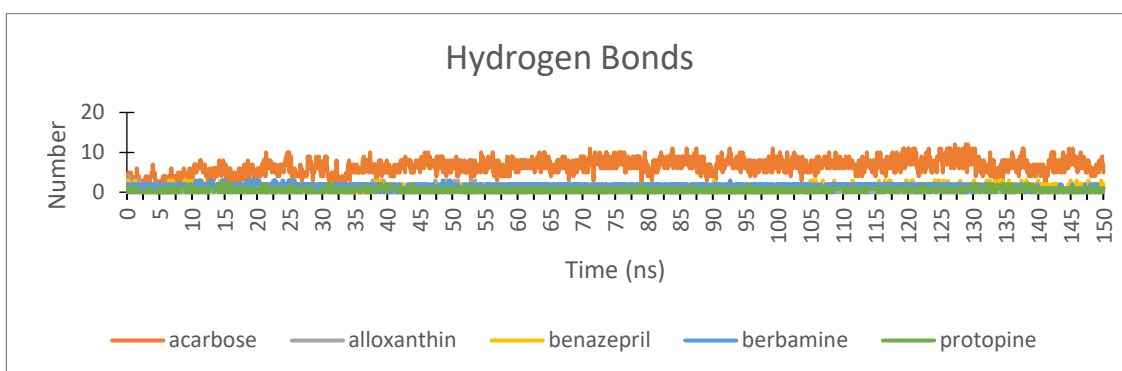


**Figure 4.7** The 2D diagram of the simulation observed the hydrogen bond patterns for the complexes

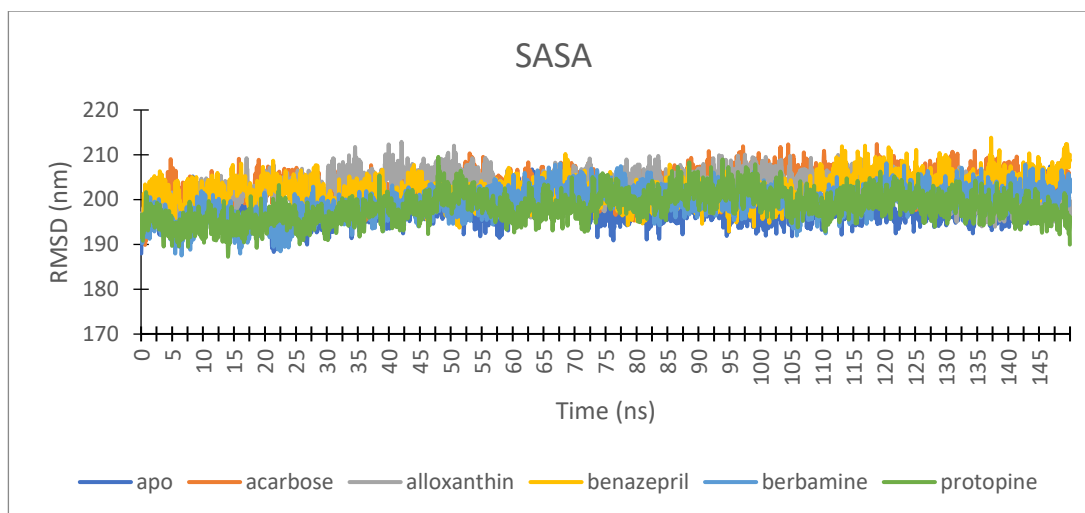


**Figure 4.8** Solvent accessible surface area (SASA) for alpha-amylase (apo) and ligands.

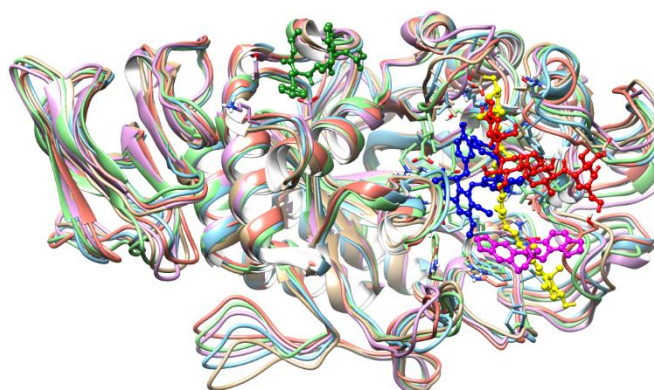


**Figure 4.9** Binding poses of the protein-ligand complex after MD simulation where Acarbose (red), alloxanthine(yellow), benazepril(green), berbamine(blue), and protopine (magenta) are seen binding on the allosteric site of alpha-amylase.

Table 4.4 indicates the generalized born surface area (GBSA) of the last 15ns. The structure of the protein-ligand complex after MD simulation has been shown in Figure 3.12, where ligands are found to bind on the allosteric site of the enzyme. Per residue decomposition as indicated in Figure 3.13 shows energy contribution of single residues by summing its interactions over all residues in the system. The MD results conclude that our screened hits from HRLCMS may be the potential inhibitors similar to the traditionally used reference compound acarbose.

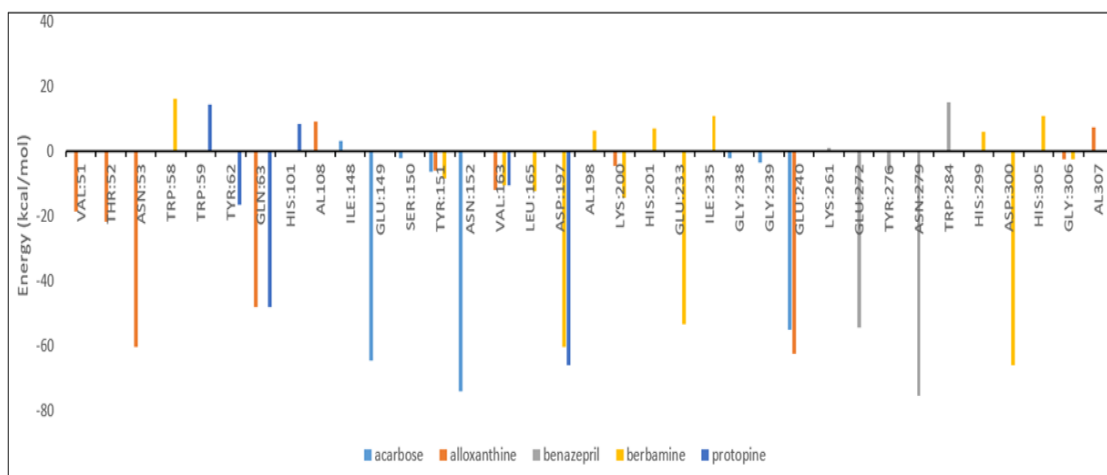


**Figure. 4.10** Per residue decomposition shows energy contribution of single residues in different ligands.

**Table 4.4** GBSA (generalized born surface area) results of the last 15ns. VDwaal- vanderwaal interaction energy, EEL (electrostatic energy), EGB (electrostatic contribution to the solvation free energy calculated by PB or GB respectively), ESURF (nonpolar contribution to the solvation free energy calculated by an empirical model), DELTA total = final estimated binding free energy calculated from the terms above. (kcal/mol).

S.no	Ligand	VDwaal (Kcal/mol)	EEL(Kcal/mol)	EGB(Kcal/mol)	Esurf (Kcal/mol)	Delta total (Kcal/mol)
1	Acarbose	-43.3016	-257.8725	251.8629	-7.5204	-56.8316
2	Alloxanthin	-50.7581	-7.52751	27.8348	-6.8995	-37.3503
3	Benazepril	-14.013	-93.399	93.4748	-2.472	-16.410
4	Berbamine	-45.834	-274.159	292.953	-5.9430	-32.9836
5	Protopine	-28.7326	-131.4275	141.055	-3.048	-22.152

#### 4.4.5 Alpha-glucosidase enzyme inhibition by *Daruharidra* extract-

The lowest IC<sub>50</sub> among the eight extracts was 17.141 mg/ml for ethanol, 27.391 mg/ml for methanol, and 26.526 mg/ml for acetone, respectively. The ethanol with the lowest IC<sub>50</sub> was

used to further investigate the kinetics of enzyme inhibition. (Table 4.5). Maltose standards were used to calculate reaction velocities at various substrate concentrations. The Lineweaver Burk plot was used to identify the mechanism of inhibition, and it indicated that it was competitive, as illustrated in Figure 4.11. Table 4.6.

**Table 4.5:** Alpha glucosidase Enzyme Inhibition concentration of different extracts (polar to nonpolar)

<b>Solvents</b>	<b>IC<sub>50</sub> mg/ml</b>
Acarbose	53.4 ± 0.01
Water	32.463 ± 0.404
Methanol	17.141 ± 0.005
Ethanol	27.391 ± 0.173
Acetone	26.525 ± 0.304
Chloroform	41.44 ± 0.286
Isopropanol	33.75 ± 0.121
Pet. ether	46.58 ± 0.201
Hexane	22.12 ± 0.317

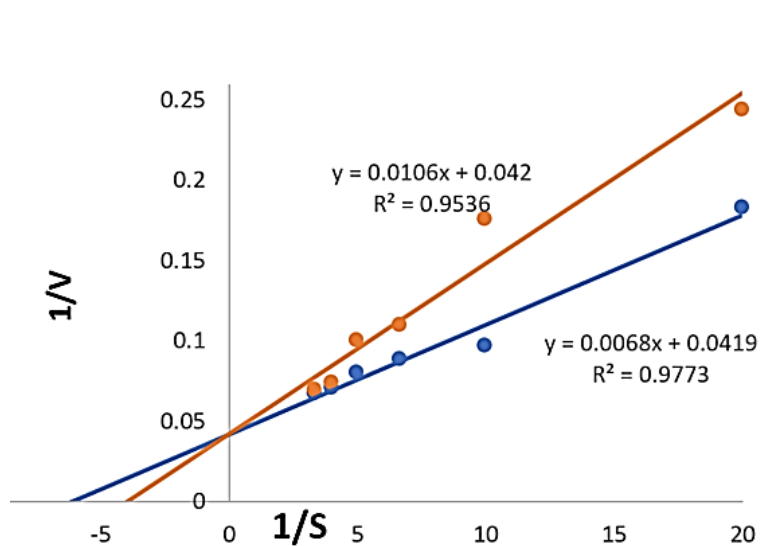


**Figure 4.11.** Lineweaver Burk plot of enzyme inhibitory activity of *Berberis aristata* DC. bark extract. Mode of inhibition of alpha glucosidase showing competitive inhibition.

The main digestive enzymes for dietary carbohydrates are intestinal glucosidases, and inhibiting these enzymes may help delay the absorption of glucose. This is due to the fact that only monosaccharides may be quickly absorbed from the gut; all other carbs must first undergo enzymatic breakdown in order to be absorbed. As compared to a typical medicine, alpha-glucosidase inhibitory potential showed that high inhibition of enzyme might lead to inconsistent microbial fermentation of unprocessed carbohydrates in the colon, which is why moderate inhibition action should be preferred as described by Priyanga et al 2015 in her experiment. When the concentration grew with both the extract and the reference acarbose, the ethanolic extracts bark extracts of inhibitory effect increased.

**Table 4.6:** Kinetic constants  $K_m$  and  $V_{max}$  for ethanolic extract of *Daruharidra* showing competitive inhibition. Control was reaction performed without inhibitor.

	<b><math>K_m</math>(mg/mL)</b>	<b><math>V_{max}</math> (<math>\mu</math>M/min)</b>	<b>Type of inhibition</b>
<b>Control (without inhibitor)</b>	0.162	23.869	
<b>Enzyme with Ethanol extract</b>	0.252	23.806	Competitive

#### 4.4.6 Analysis phytoconstituents for their drug likeness prediction by ADMET Test-

To ascertain the drug likeness probability index of ligands, this test was conducted. For a lead compound to be used as a drug it needs to qualify some basic criteria that will qualify it as an effective drug. In an attempt to improve the quality of private chemical collections, Swiss ADME filters chemical libraries using five distinct rule-based filters from large pharmaceutical companies. This is done by removing molecules that have properties that are inconsistent with a decent pharmacokinetics profile. The five pioneer rules: Molecular weight (MW) < 500, MLOGP  $\leq$  4.15, N or O  $\leq$  10, NH or OH  $\leq$  5, and the Lipinski filter (Pfizer) are used to characterize small molecules based on their physicochemical property profiles. According to Lipinski, all nitrogen and oxygen are strictly considered H-bond donors, but all nitrogen and oxygen that contain at least one hydrogen are considered H-bond acceptors. Alanine nitrogen is neither a donor nor an acceptor, whereas aliphatic fluorines are acceptors as described by lipinski. All of the ligands utilised in the trials had high GI absorption and excellent bioavailability, it was discovered. Table 4.7 shows that the ligands' high to moderate water solubility resulted in minimal toxicity.

**Table 4.7:** ADMET analysis of HRLCMS hits as leads for their drug likelihood.

Ligand	PubChem ID	Molecular weight (g/mol)	Lipinski likeness	LD50 (mg/kg)	Skin permeation (log K <sub>p</sub> cm/s)	Bio-availability	Water-soluble	GI abs.
Acetoxylkivorin	76311434	644.7	NO	244	-5.05	0.17	Moderate	Low
Berbamine	275182	608.2	YES	1700	-8.22	0.55	Poor	High
Ambelline	25092366	331.4	YES	86	-7.44	0.55	High	High
Desmethylnefopam	601526	239.31	YES	80	-7.44	0.17	Moderate	High
Desmethylverapamil	625729	440.6	YES	108	-6.53	0.55	Moderate	High
Dihydrosphingosine	91486	301.5	YES	3500	-4.02	0.55	Moderate	High
Ethambutol aldehyde	14052	204.31	YES	998	-7.60	0.55	High	High
Evoxine	73416	347.4	YES	1000	-6.89	0.55	High	High
Naloxol	44230574	329.4	YES	359	-7.30	0.55	High	High
Oxycodone	5284603	315.4	YES	402	-8.90	0.55	High	High
Pirenzepine	4848	351.4	YES	500	-8.37	0.55	Moderate	High
Platyphylline	5281742	337.4	YES	2573	-6.99	0.55	High	High
Procainamide	4913	235.33	YES	525	-7.11	0.55	High	High
Prometon	4928	225.29	YES	433	-5.55	0.55	High	High
Scopolamine	2837667	339.8	YES	1275	-7.45	0.55	High	High
Tiagabine	60648	375.6	YES	867	-6.36	0.55	Moderate	High
Vinblastine	13342	811	NO	68	-8.49	0.17	Poor	Low
Dihydroartemisinin	3000518	284.35	YES	567	-7.61	0.55	High	High
Chelidonium	197810	353.4	Yes	460	2.26	0.55	Moderately	High
Benazepril	5463984	396.4	Yes	4019	2.43	0.55	Poorly	High
Protopine	4970	353.4	Yes	940	2.67	0.55	Moderately	High

#### 4.4.7 Molecular Docking of enzyme 5KZX with HRLCMS encountered ligand -

Its alpha-glucosidase enzyme's active site was docked with all of the ligands. The in vitro investigation indicates that extract of *Daruharidra* exhibits competitive inhibition. The alpha-glucosidase enzyme was docked to determine the binding energies of all the alkaloid hits found in HRLCMS. The binding energy for the ideal blind docking position was noted and is shown in Table 4.8 as an expression. The least binding energy among the positions was taken into consideration to determine the optimal binding pose.[162]

Figure 4.12 illustrates the optimal pose by taking pictures of the relevant amino acids and hydrogen bonds. When compared to other ligands, pirenzepine has the highest binding affinity to the alpha-glucosidase enzyme. It interacts with many residues and binds with TRP 481 through hydrogen ions. It was discovered that the binding energy value was -9.40 kcal/mol.

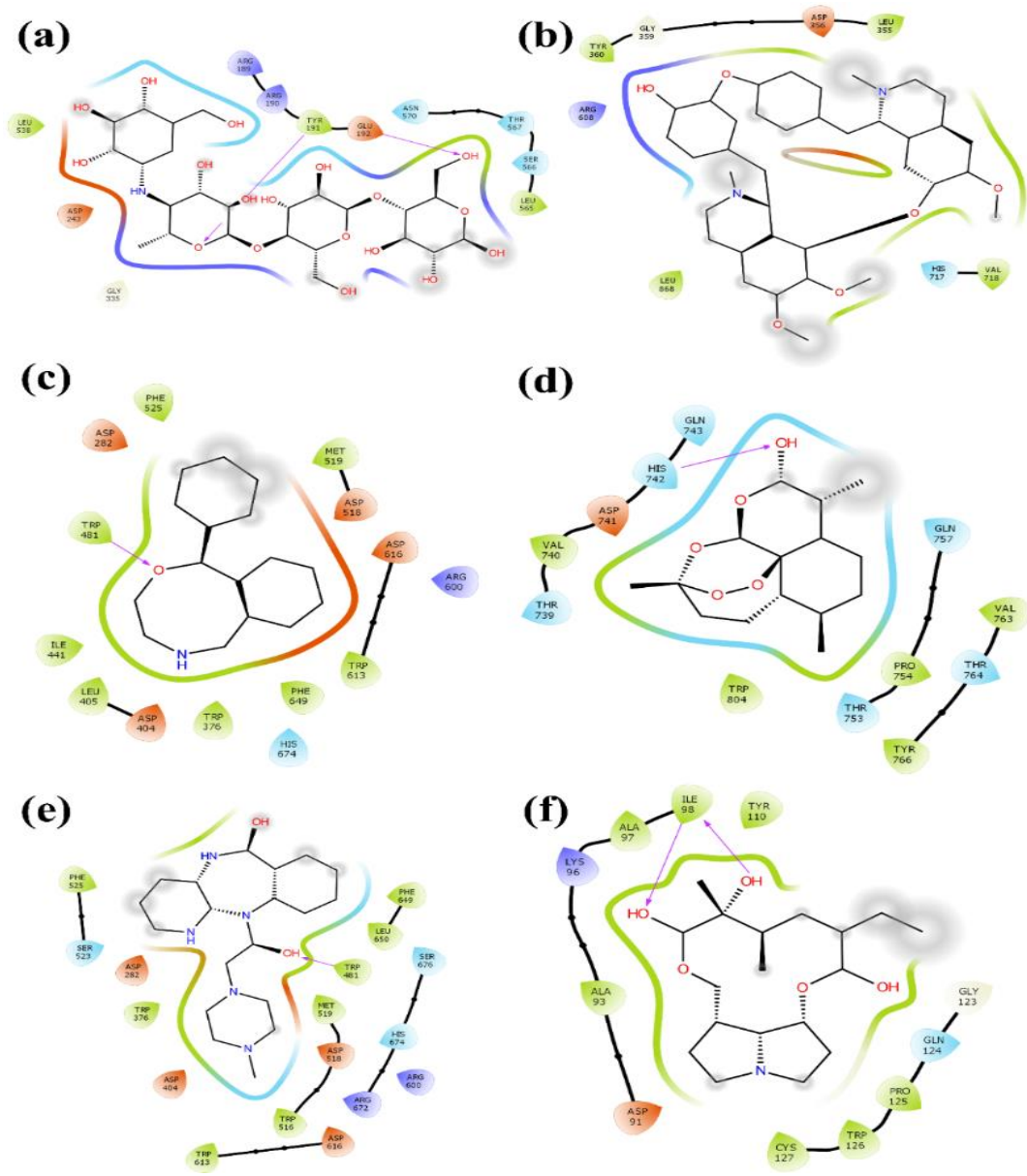


**Figure 4.12:** Docking images of ligands having most negative binding energy where (a) Acarbose (b) berbamine (c) desmethylnefopam (d) dihydrostermisinin (e) pirenzepine (f) platyphylline.

**Table 4.8.** Results of docking of metabolites on alpha-glucosidase enzyme (5KZX).

<b>Ligands</b>	<b>Binding energy (kcal/mol)</b>	<b>H bonds</b>	<b>Amino acids</b>
Acarbose	-4.76	4	GLN603, TYR605, ASP642, HIS600
Acetoxymorphine	-6.87	1	ARG608
Berbamine	-7.65	1	TYR360
Ambelline	-7.52	1	VAL236
Desmethylnepomam	-7.74	1	TRP481
Desmethylverapamil	-5.26	2	SER924, CYS938
Dihydrosphingosine	-2.55	2	TYR360, ARG608
Ethambutol	-7.08	2	HIS674, ASP616
Evoxetine	-4.76	1	ASP616
Naloxol	-6.73	4	ASP91, GLY123, CYS127, ILE98
Oxycodone	-6.90	3	ASP243, TYR191, GLY335
Pirenzepine	-9.40	1	TRP481
Platyphylline	-7.73	1	ILE98
Procainamide	-5.58	2	ASP616, TRP481
Prometon	-7.63	3	TRP481, ASP616, ARG600
Scopolamine	-6.81	3	GLU866, ARG608, MET363
Tiagabine	-7.04	2	ARG331, ASP91
Vinblastine	-6.05	1	HIS584
Dihydroartemisinin	-8.11	3	SER924, MET363, VAL867

#### 4.4.8 Simulation studies-

To assess the structural stability of the complexes as indicated above in the methodology, MD simulation analysis using alpha-glucosidase and ligands was performed, with acarbose serving as the control. Structure changes in complex and dynamic behaviour were investigated using the RMSD, hydrogen bond, RG, RMSF and SASA computations.

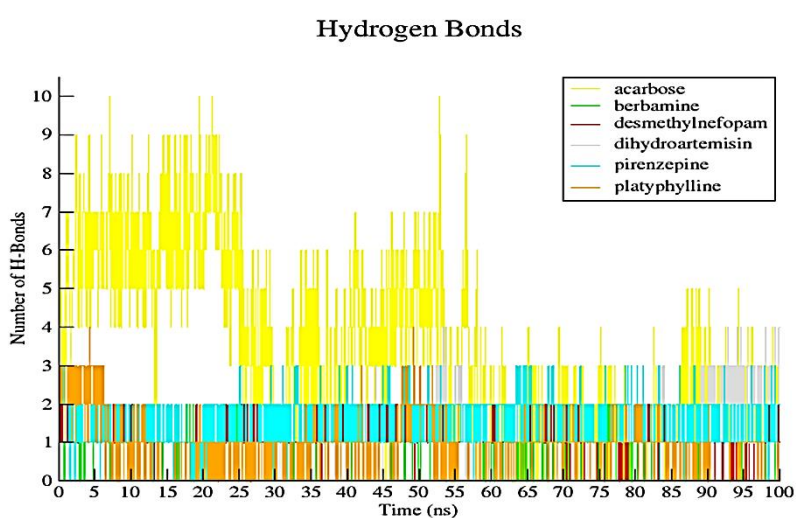
For all complexes for the 100 ns trajectory, the RMSD, SASA and RMSF plot of natural alpha-glucosidase and protein-ligand complexes (Figure 4.14) was determined. Acarbose has a low RMSD standard, according to simulation studies, indicating strong binding between the ligand and receptor alpha-glucosidase.

As evident by overlapping RMSD values we can be assured of the tight binding of ligands to protein complex, in which pirenzepine has close to control binding. Protein backbone atom structural and conformational changes were investigated using RMSD calculations. The RMSD graph for the protein-ligand complexes and apoprotein is displayed in Figure 4.15. The  $\alpha$ -glucosidase backbone atoms' RMSD analysis verified that every protein ligand complex and apoprotein demonstrated strong stability over the course of the 100 ns simulation. They behaved in the same way as the protein-acarbose combination used as a reference. Acarbose gets stabilized after 10 ns, and others are shown to get stable after 40ns.

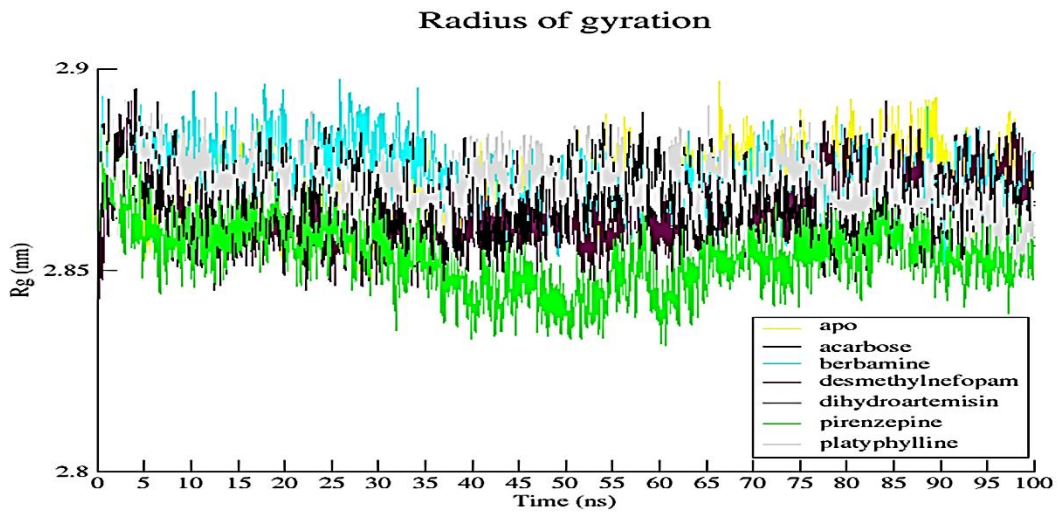
The radius of gyration value was calculated by using a 100 ns trajectory. Figure 4.14 shows the plot of average RG as a function of time for native protein and all the  $\alpha$ -glucosidase-ligand complexes.[163] The protein's stability and the complexes that stay folded or unfolded during simulation are shown by the Radius of Gyration. It is a metric for how compact a complex is. The complex's radius of gyration with time is seen in Figure. 4.14. All of the complexes' and the native proteins' radii of gyration were extremely comparable to one another and overlaid, suggesting that the proteins stayed compact and folded throughout the simulation. The average Rg value was 2.85 nm. This demonstrated how the active phytochemicals increased the protein's stiffness during the simulation.

For the enzyme  $\alpha$ -glucosidase, variations in the component residues were noted, and all protein-ligand complexes were shown in Figure 4.16 as a function of time over 100 ns trajectories of MD simulation. Similar RMSF values and variations in the same residues were seen in all of the complexes. The protein stayed rigid during the simulation and had more helix and sheets

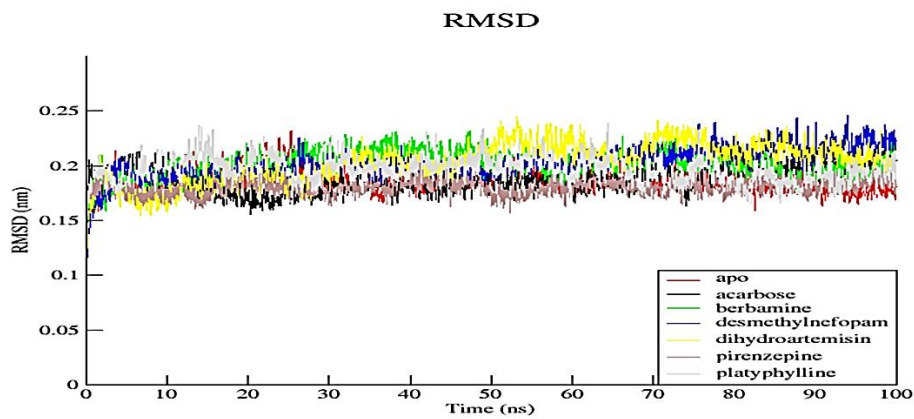
in the secondary structure, as indicated by the average RMSF value of all the  $\alpha$ -Glucosidase-ligand complexes being substantially smaller and the same as acarbose. The magnitude of the conformational changes resulting from the contact is predicted by the SASA computation. All of the protein alpha-glucosidase -ligand complexes' H bond and SASA values are shown against time in Figures 4.13 and 4.14, respectively. As illustrated in Figure.4.14, every ligand- $\alpha$ -Glucosidase complex displayed almost identical SASA values (315.4–343 nm<sup>2</sup>) to the acarbose- $\alpha$ -Glucosidase complex (330.5 nm<sup>2</sup>). As a result, the outcomes of the molecular dynamic simulation demonstrated that throughout the 100-ns simulation, every complex was extremely rigid, compact, and folded. Consequently, the *Daruharidra* phytochemicals that have been examined may be able to block alpha-glucosidase proteins, such as acarbose, and may offer a promising avenue for the treatment of diabetes. Figure 4.16 depicts the structure of the protein-ligand complex following MD simulation, where it is discovered that ligands attach to the enzyme's active site. According to the MD findings, our HRLCMS screening hits may represent potential inhibitors that are comparable to the commonly used reference drug acarbose.



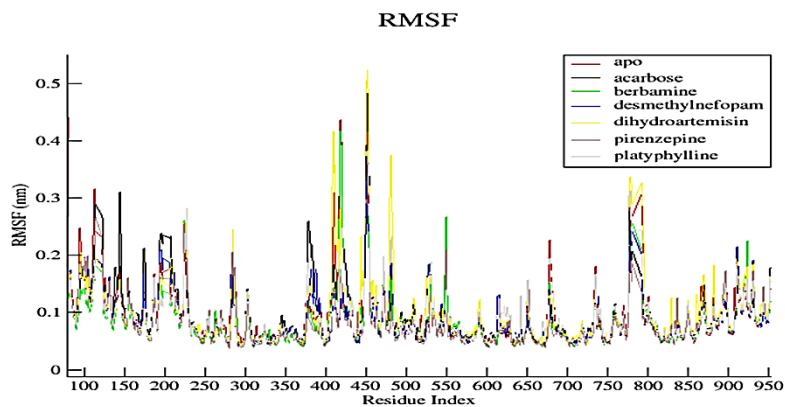
**Figure 4.13** Hydrogen bonds pattern observed in simulation after 100 ns.

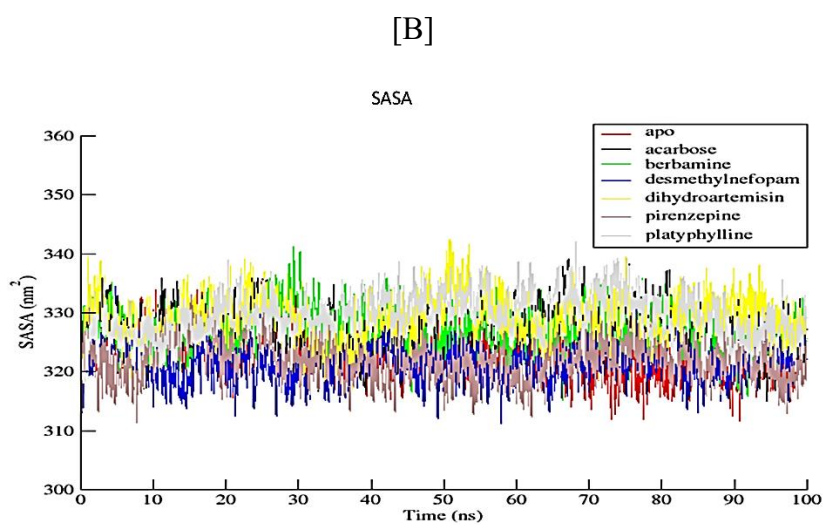


**Figure 4.14:** Observed conformational changes in radius of gyration during simulation between enzyme and ligand complex.



[A]





[C]

**Figure 4.15:** (A) RMSD, (B) RMSF and (C) SASA of the ligands and alpha glucosidase complex showing the comparable results with positive control Acarbose.

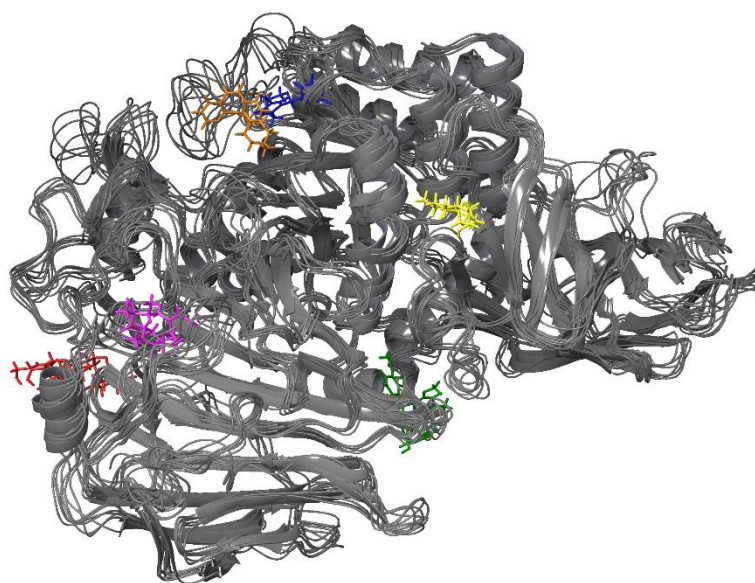


**Figure 4.16.** Image of alpha glucosidase with all the ligands after simulation. Acarbose: red, Berbamine: green, Desmethnefopam: blue, Dihydroartemisinin: yellow, Pirenzepine: orange, Platyphylline: pink.

#### 4.5 Conclusion-

The purpose of the current study was to investigate a well-known Indian ayurvedic herb *Daruharidra* possessing novel leads for the treatment of diabetes. A systematic study was carried out on the *Daruharidra* plant to evaluate its anti-diabetic potential via inhibition of the alpha-amylase enzyme. It is a known enzyme in carbohydrate metabolism, and *Daruharidra* is used in ancient scriptures as a multipurpose plant having therapeutic value. Enzyme assay showed non-competitive inhibition of the enzyme, which makes way for further investigation about active constituents and, thus, a new herbal medicine for diabetes. It was observed from in silico screening, and result from analysis berbamine, benazepril, alloxanthine, and protopine have substantial anti-diabetic potential and proves the results of in vitro non-competitive inhibition. Since many synthetic drugs are present for treating diabetes, they come along with numerous side effects. These phytochemicals can be utilized in the clinical treatment of diabetes. Using herbal remedies such as *Daruharidra* could be an alternative therapy for diabetes.

Therapeutic properties of the plant were investigated to inhibit the well-known glucose metabolizing enzyme. i.e., alpha glucosidase. Hits encountered in HRLCMS were found to act in vitro as a competitive inhibitor of the enzyme which was also proved in the docking and molecular dynamic simulation studies. The plant is known to be rich in alkaloids and therefore the hits having alkaloid nature were mainly targeted for the inspection of their role in enzyme inhibition. The results from this article are quite promising for the use of *Daruharidra* plant to treat the disease of concern. Future experiments could be drafted in a way to navigate more plausible advantages of *Daruharidra* as tool to treat diabetes mellitus. This plant's marvellous medicinal value needs to be researched robustly. Studies should be focussed to develop herbal and ayurvedic formulations that are less toxic and have fewer side effects.